S1. Formaldehyde nitrogen ratio (FNR)

For discussion of ozone (O_3) sensitivity to its precursors, the formaldehyde nitrogen ratio (FNR) (Jin and Holloway, 2015) is used to feature the O_3 formation regime, with FNR<1.0 representing VOC-limited regimes, FNR> 2.0 representing NO_x-limited regime, and FNR between 1.0 and 2.0 representing transitional regime. For model evaluation, monthly mean Aqua OMI tropospheric columns of nitrogen dioxide (NO_2) (Boersma et al., 2011) and formaldehyde (HCHO) (De Smedt et al., 2015) products in 2015 are obtained from https://www.temis.nl/airpollution/, with resolutions of 0.125° × 0.125° and 0.25° × 0.25°, respectively. The satellite observations are interpolated into 2° × 2.5° resolution to be consistent with that of model outputs. Figure S6 evaluates the simulated present-day tropospheric columns of NO_2 and HCHO in CpdEpd simulation by comparing with Aqua satellite observations. The tropospheric columns of NO_2 and HCHO levels are overestimated by 4.4 and 1.1 10^{15} molec cm^{-2} in EC and by 1.8 and 0.7 10^{15} molec cm^{-2} nationwide, respectively. The overestimation of tropospheric columns of NO_2 and HCHO can be attributed to the lower tropopause pressure in GCAP 2.0 simulations (Murray et al., 2021).

Table S1. Information of climate models in CMIP6 used in this study.

Model	N	Member_id (Historical/SSP1-1.9)
CanESM5	2	r1i1p1f1, r1i1p2f1
GFDL-ESM4	1	r1i1p1f1
GISS-E2-1-G[a]	3	r1i1p1f2, r1i1p3f1, r1i1p5f1
GISS-E2-1-H[b]	2	r1i1p1f2, r1i1p3f1
MIROC-ES2H	1	r1i1p4f2
MIROC-ES2L	1	r1i1p1f2
Total	10	

[a, b] GISS-E2.1-G and GISS-E2.1-H are coupled models of the GISS-E2.1 atmospheric model with the GISS and HYCOM ocean models, respectively.

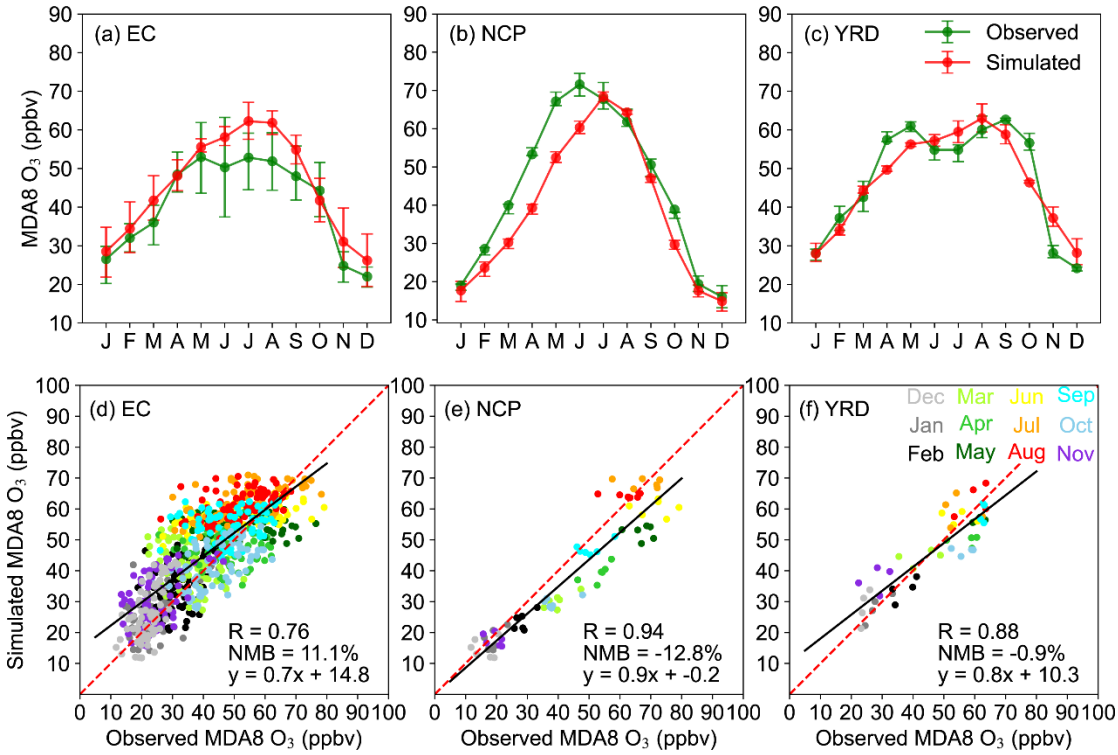

Figure S1. (a)-(c) Monthly variations in simulated and observed MDA8 O_3 concentrations (ppbv) over (a) EC (with a total of 68 grids), (b) NCP (with a total of 6 grids), and (c) YRD (with a total of 4 grids) regions. Bars represent the range from first to third quartiles of all grid samples in this region. (d)-(f) The scatterplot of simulated versus observed monthly mean MDA8 O_3 concentrations for grids in EC, NCP, and YRD. The linear fit (black solid line and equation), correlation coefficient (R), and normalized mean biases (NMB) that calculated for grids in these three regions are also shown when all of the year 2015 data are considered.

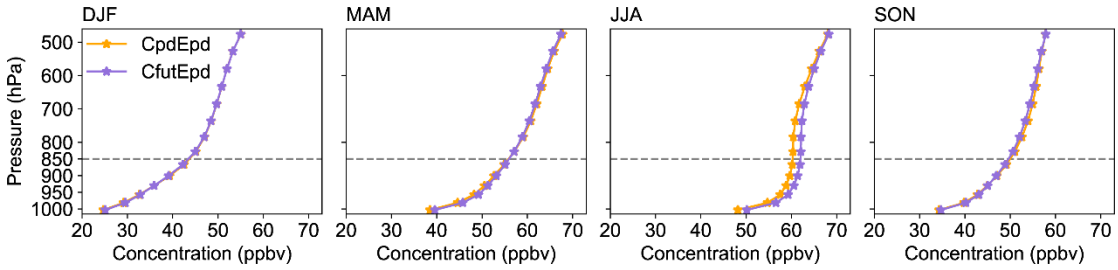

Figure S2. Vertical profile of seasonal mean O_3 concentrations (ppbv) over EC in CpdEpd and CfutEpd simulations.

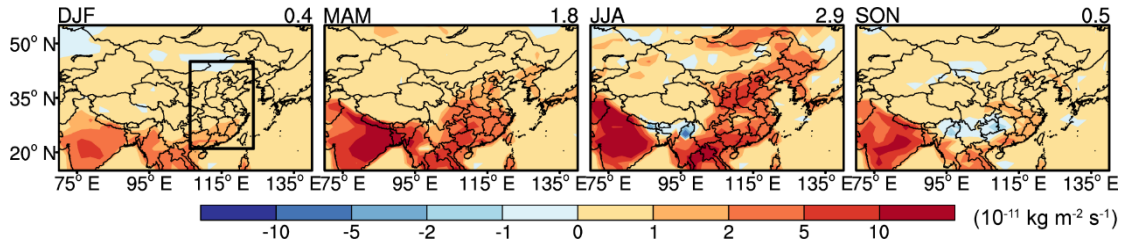

Figure S3. Seasonal mean changes in biogenic emission rates of VOCs (10^{-11} kg m^{-2} s^{-1}) due to climate change over 2010-2045. The black rectangle indicates the domain of EC, and the top right number of each panel is the regional mean value for EC.

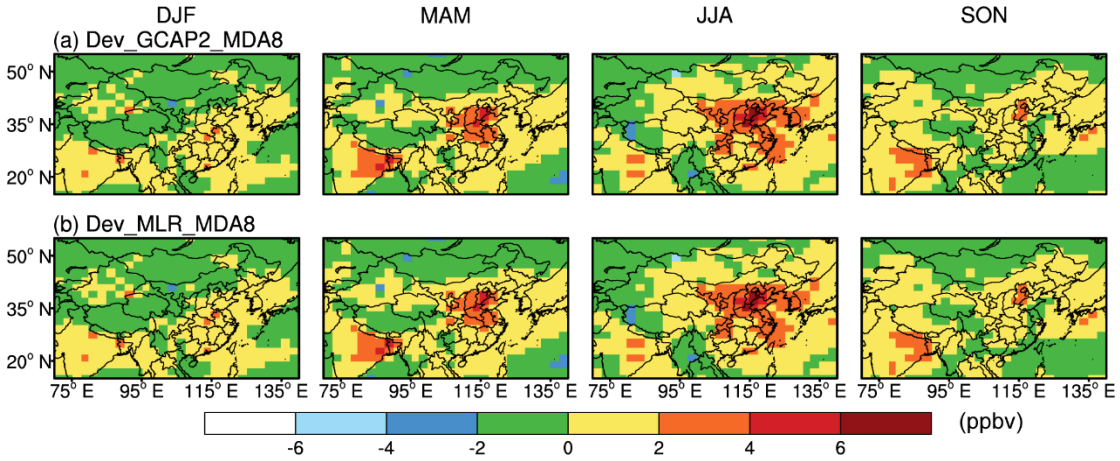

Figure S4. Comparisons of the spatial distributions of climate-induced seasonal mean MDA8 O_3 changes simulated by (a) GCAP 2.0 (Dev_GCAP2_MDA8) with those predicted by (b) stepwise MLR model (Dev_MLR_MDA8).

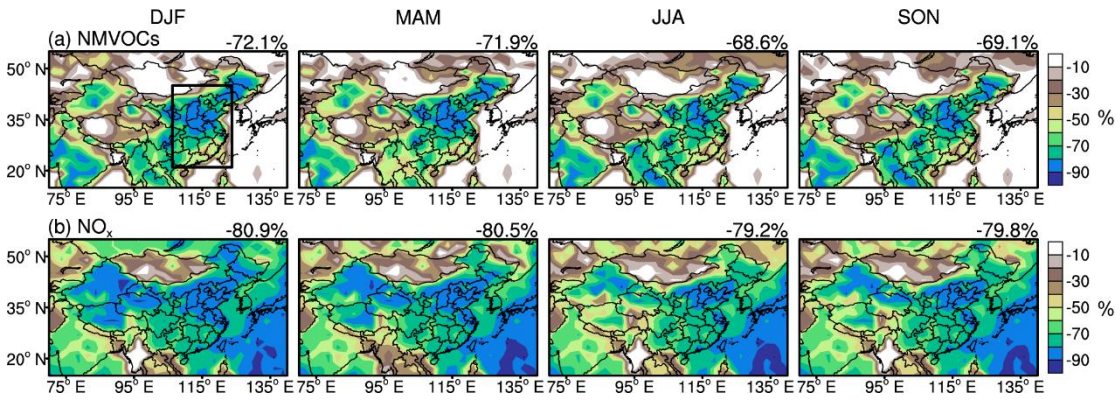

Figure S5. Percentage changes (%) in anthropogenic emission rates of (a) NMVOCs and (b) NO_x in 2050 relative to 2015 under SSP1-1.9 scenario. The black rectangle indicates the domain of EC, and the top right number of each panel is the regional mean value for EC.

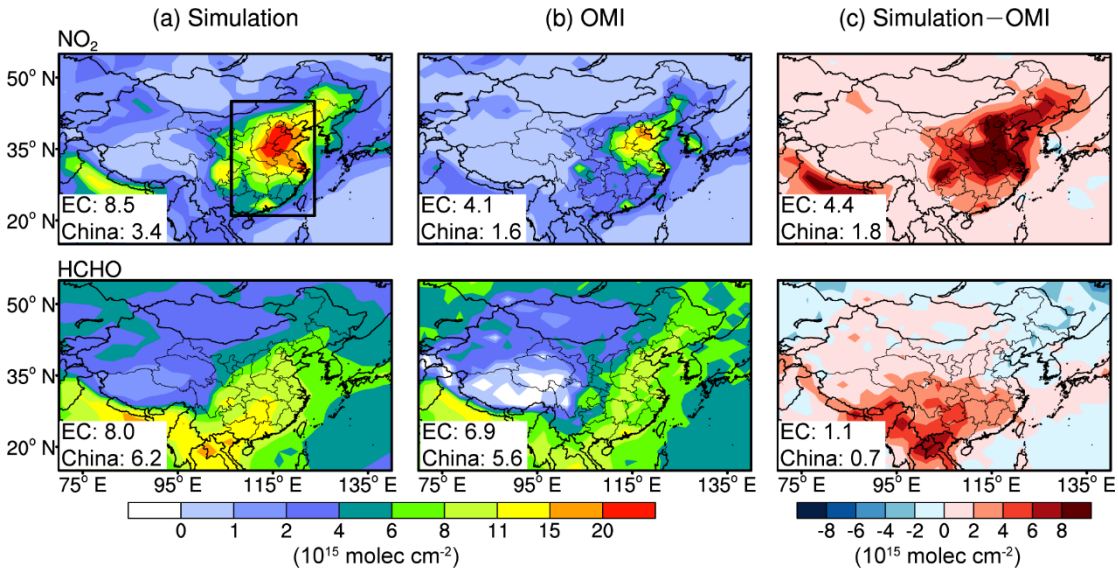

Figure S6. (a) Simulated and (b) OMI retrieved annual mean tropospheric columns of nitrogen dioxide (NO_2) and formaldehyde (HCHO) (10^{15} molec cm^{-2}) in 2015 in China, and (c) their difference. The black rectangle indicates the domain of EC, and the regional mean values for EC and the whole country are shown in the bottom left corner of each panel.

References

Boersma, K. F., Eskes, H. J., Dirksen, R. J., van der A, R. J., Veefkind, J. P., Stammes, P., Huijnen, V., Kleipool, Q. L., Sneep, M., Claas, J., Leitão, J., Richter, A., Zhou, Y., and Brunner, D.: An improved tropospheric NO_2 column retrieval algorithm for the Ozone Monitoring Instrument, Atmos. Meas. Tech., 4, 1905-1928, https://doi.org/10.5194/amt-4-1905-2011, 2011.

De Smedt, I., Stavrakou, T., Hendrick, F., Danckaert, T., Vlemmix, T., Pinardi, G., Theys, N., Lerot, C., Gielen, C., Vigouroux, C., Hermans, C., Fayt, C., Veefkind, P., Müller, J. F., and Van Roozendael, M.: Diurnal, seasonal and long-term variations of global formaldehyde columns inferred from combined OMI and GOME-2 observations, Atmos. Chem. Phys., 15, 12519-12545, https://doi.org/10.5194/acp-15-12519-2015, 2015.

Jin, X. and Holloway, T.: Spatial and temporal variability of ozone sensitivity over China observed from the Ozone Monitoring Instrument, J. Geophys. Res.: Atmos., 120, 7229-7246, https://doi.org/10.1002/2015jd023250, 2015.

Murray, L. T., Leibensperger, E. M., Orbe, C., Mickley, L. J., and Sulprizio, M.: GCAP 2.0: a global 3-D chemical-transport model framework for past, present, and future climate scenarios, Geosci. Model Dev., 14, 5789-5823, https://doi.org/10.5194/gmd-14-5789-2021, 2021.